

A Hierarchical Feature Engineering Framework for Automated Classification of Phonotraumatic and Non-Phonotraumatic Vocal Hyperfunction

June-Woo Kim^{1,2,3}, Kangwook Jang⁴, Minu Kim⁴, Hyunju Lee^{† 3,5}

¹ Department of Electronic Engineering, Wonkwang University, Republic of Korea

² AI Convergence Research Institute, Wonkwang University, Republic of Korea

³ GIST InnoCORE AI-Nano Convergence Institute for Early Detection of Neurodegenerative Diseases, Gwangju Institute of Science and Technology, Republic of Korea

⁴ School of Electrical Engineering, KAIST, Republic of Korea

⁵ Department of AI Convergence, Gwangju Institute of Science and Technology, Republic of Korea

kaen2891@wku.ac.kr, hyunjulee@gist.ac.kr

Abstract

Ambulatory neck-surface acceleration enables non-invasive monitoring of vocal hyperfunction, yet robust biomarkers for its subtypes remain limited. This study investigates the NeckVibe Challenge dataset to distinguish phonotraumatic (PVH) and non-phonotraumatic (NPVH) from healthy controls. We propose a hierarchical feature engineering framework comprising: (i) static, (ii) dynamic, (iii) ratio-based, (iv) coupling features capturing source filter interactions. While univariate statistical analysis shows strong separability for PVH but limited significance for NPVH, our machine learning pipeline, tailored for high-dimensional feature integration, identifies that coupling features are crucial for both tasks. We achieve an AUC of 0.891 for PVH and 0.728 for NPVH, suggesting that while PVH is near-linearly separable, NPVH discrimination benefits from modeling non-linear feature interactions.

Index Terms: vocal hyperfunction, ambulatory voice monitoring, feature engineering, acoustic and aerodynamic measures

1. Introduction

Vocal hyperfunction (VH) is a prevalent condition characterized by chronic voice misuse, leading to disorders categorized as phonotraumatic VH (PVH, e.g., nodules) and non-phonotraumatic VH (NPVH, e.g., muscle tension dysphonia) [1, 2]. While clinical diagnosis is standard, ambulatory monitoring using neck-surface acceleration (ACC) has emerged as a powerful tool for capturing daily vocal behavior in naturalistic settings [3, 4, 5, 6]. However, distinguishing PVH subtypes from healthy controls remains challenging due to the high variability of acoustic and aerodynamic measures in daily life [7].

Recent studies have utilized various features derived from ACC signals, such as aerodynamic measures estimated via Impedance-based Inverse Filtering (IBIF) [8] to quantify glottal airflow [5, 6, 7, 9, 10]. While these measures provide insights into vocal fold physiology, most approaches rely on simple time-averages of individual features, potentially overlooking the dynamic and interdependent nature of speech production [11]. In particular, the *physiological coupling* between different vocal parameters, such as the relationship between aerodynamic effort and acoustic output is often neglected in automated classification pipelines [10, 12].

Here, we investigate the NeckVibe Challenge dataset to improve PVH and NPVH classification. Our contributions are:

- We propose a hierarchical feature engineering framework categorized into static distributions, dynamic trend descriptors, ratio-based proportions, and physiologically motivated coupling features to capture the complex mechanism of vocal hyperfunction.
- We perform rigorous univariate statistical analysis using Welch’s t-test with Benjamini-Hochberg false discovery rate (FDR) [13] correction to identify features that distinguish PVH and NPVH, providing clinical interpretability.
- We employ a recursive feature elimination cross-validation (RFECV) pipeline to demonstrate that while PVH is near-linearly separable, NPVH classification benefits significantly from capturing non-linear feature interactions through our proposed feature set.
- We validate our framework using a stratified 10-fold group cross-validation on the given NeckVibe Challenge dataset. The model achieves an AUC of 0.891 for Task 1 (PVH vs. Control) and 0.728 for Task 2 (NPVH vs. Control), providing a competitive baseline and demonstrating the practical utility of our hierarchical features for biomarker identification in vocal hyperfunction.

2. NeckVibe Challenge Dataset

The NeckVibe Challenge provides ambulatory neck surface acceleration-derived measurements for subject-level voice disorder detection. The challenge defines two binary classification tasks: (i) PVH versus PVH Control and (ii) NPVH versus NPVH Control. The dataset comprises 3,278 samples from 468 subjects. Specifically, PVH includes 1,151 samples from 171 subjects, and PVH Control includes 992 samples from 136 subjects. NPVH includes 637 samples from 93 subjects, and NPVH Control includes 498 samples from 68 subjects. IBIF-based aerodynamic variables are partially missing for a subset of subjects and samples: 9 subjects have missing IBIF measurements in at least one recording (PVH: 6, NPVH: 2, NPVH Control: 1), corresponding to 55 samples with missing IBIF (PVH: 37, NPVH: 11, NPVH Control: 7), while PVH Control has no missing IBIF.

As shown in Table 1, the dataset comprised of 14 core physical quantities, consisting of six acoustic measures and eight IBIF-based aerodynamic measures. Each frame includes a voiced indicator, and we restrict feature computation to voiced frames to focus on phonatory segments. For statistical analyses, observations containing imputed or missing values were

[†]Corresponding author.

Table 1: Core acoustic and aerodynamic (IBIF-derived) features extracted from neck-surface acceleration signals.

Category	Variable	Description (Unit)
Acoustic	H1H2all	Harmonic magnitude difference between H1 and H2; reflects glottal configuration (dB)
	LHratioall	Low/high frequency power ratio (70–2000 Hz vs. 2000–3730 Hz); spectral balance (dB)
	cppall	Cepstral peak prominence; periodicity and dysphonia measure (dB)
	dBcms2	RMS neck-surface acceleration amplitude (dB re cm/s^2)
	level	Log-scaled RMS neck-surface acceleration amplitude (dB re cm/s^2)
Aerodynamic (IBIF)	spectralTiltall	Spectral tilt; regression slope across first eight harmonics (dB/oct)
	IBIF_h1h2	Harmonic magnitude difference H1–H2 from estimated airflow (dB)
	IBIF_hrf	Harmonic richness factor; summed harmonics relative to first harmonic (dB)
	IBIF_mfdr	Maximum flow declination rate; peak negative airflow derivative (L/s^2)
	IBIF_acflow	Peak-to-peak glottal airflow amplitude (mL/s)
	IBIF_sq	Speed quotient (ratio of opening to closing phase duration) (unitless)
	IBIF_oq	Open quotient; proportion of glottal cycle open (unitless)
	IBIF_naq	Normalized amplitude quotient; ACFL/MFDR normalized by period (unitless)
	IBIF_cq	Closing quotient; proportion of glottal cycle in closing phase (unitless)

excluded to avoid bias in group-level differences. In contrast, for machine learning (ML) experiments, missing values were processed using median imputation within each training fold.

3. Methods

3.1. Feature Construction

To capture the complex mechanisms of VH, we constructed a hierarchical feature set focusing on static, dynamic, ratio-based, and coupling properties. We include the *vocal dose percentage* in all configurations, defined as the proportion of voiced frames relative to total recording time. All frame-level measures were aggregated to subject-level representations.

Static Features. For each core acoustic and IBIF variable, seven statistical descriptors were computed to characterize central tendency, variability, and distributional shape: mean, standard deviation (SD), 5th percentile (P_5), 95th percentile (P_{95}), skewness, kurtosis, interquartile range. The total number of static features is $14 \times 7 + 1 = 99$, where 14 denotes the number of base features with the vocal dose percentage.

Dynamic Features. Temporal dynamics were modeled using first-order (Δ) and second-order ($\Delta\Delta$) differences statistics, including delta mean, delta SD, upper-tail delta magnitude (P_{95}), mean absolute delta, delta–delta SD, and linear trend (slope). The dynamic feature configuration consists of 14×7 additional descriptors combined with the static features, resulting in a total of 197 features.

Ratio-based Features. To obtain normalized representations, four additional relative variability measures were computed for each base feature: $\Delta\text{SD}/\text{mean}$, $\Delta\text{SD}/\text{SD}$, $|\text{slope}|/\text{mean}$, and $|\Delta|/\text{mean}$. These descriptors quantify temporal variability relative to absolute level or dispersion. The ratio-based configuration therefore adds 14×4 features to the dynamic feature set, resulting in a total of $14 \times 4 + 197 = 253$ features.

Coupling Features. Six physiologically motivated [10, 12] interaction terms were introduced to capture relationships between acoustic and aerodynamic properties. These include source-filter coupling (cppall/spectralTiltall, cppall/H1H2all), stability-effort coupling (cppall/ ΔSD , cppall/abs Δ), and aerodynamic intra-feature coupling (IBIF_naq/ ΔSD , IBIF_oq/abs Δ). The coupling configuration extends the dynamic feature set by six interaction terms, resulting in a total of $197 + 6 = 203$ features.

3.2. Univariate Statistical Analysis

Statistical comparisons were performed for each task (Task 1 vs. Task 2). Group differences were assessed independently using *Welch’s t-tests*, which do not assume equal variances or sample sizes. The magnitude of group differences was quantified using *Cohen’s d* effect size. To control for Type I errors in high-dimensional testing, *p*-values were adjusted using the *Benjamini–Hochberg FDR* procedure within each feature set.

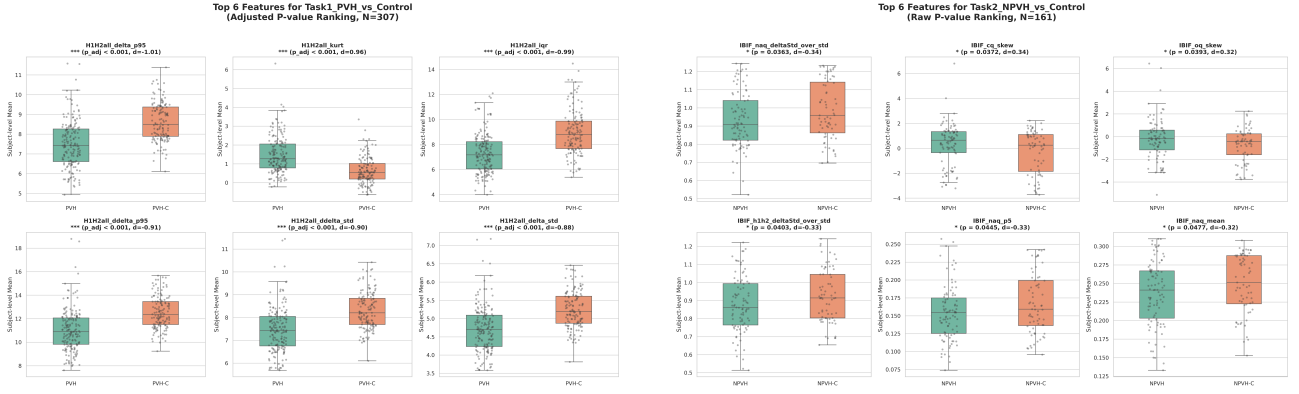
3.3. Machine Learning Analysis

Cross-Validation Strategy by Subject-Level. We conducted supervised classification experiments at the subject level to determine whether multivariate modeling could capture interaction patterns beyond univariate statistical differences. All experiments were performed separately for PVH vs. PVH Control (Task 1) and NPVH vs. NPVH Control (Task 2), using the same subject-level feature representations described in the previous section. We implemented a stratified 10-fold CV scheme using subject IDs as grouping variables which guarantees that all acoustic recordings from a specific individual are strictly confined to either the training or validation set within each fold.

Feature Selection by ML Models. To further address high-dimensional feature space redundancy and enhance model stability, we performed automatic feature selection exclusively within these designated training folds motivated by work in schizophrenia screening [14]. Specifically, RFECV utilizing an XGBoost tree-based estimator was applied. While we also evaluated a preliminary greedy search algorithm, it yielded sub-optimal classification performance. Consequently, the optimal feature subset identified via RFECV was utilized consistently across all subsequent classifier evaluations.

Classification Models. Five ML classifiers were evaluated: logistic regression [15], support vector machine (SVM) with Gaussian kernel [16], random forest [17], XGBoost [18], lightGBM [19]. The experimental design was intended to compare statistical feature representations under controlled conditions. The primary objective was to assess how different feature structures influence classification performance, rather than to optimize predictive accuracy through extensive hyperparameter search. Accordingly, fixed hyperparameter configurations were used and applied across folds and feature sets.

Model Interpretations. To analyze feature contribution patterns and model behavior, SHapley Additive exPlanations (SHAP) [20] were computed for the best-performing model in each task using a model-agnostic explainer. SHAP values were



(a) Task 1 (PVH vs. Control). Top six subject-level features ranked by FDR-adjusted p -value. All displayed features remain statistically significant after multiple comparison correction ($p_{adj} < 0.001$), with large effect sizes ($|d| \approx 0.9-1.0$).

(b) Task 2 (NPVH vs. Control). Top six subject-level features ranked by raw p -value. No features survived FDR correction; features with nominal significance ($p < 0.05$) are shown to illustrate exploratory trends. Effect sizes are smaller than Task 1 ($|d| \approx 0.3$).

Figure 1: Comparison of statistical features for PVH (Task 1) and NPVH (Task 2). While PVH exhibits robust group separation characterized by large effect sizes across multiple dynamic and higher-order statistics, NPVH shows only weak and inconsistent differences at the daily summary level, even among the most discriminative features.

Table 2: Summary of statistically significant features across different feature configurations for each task. **Task 1 Sig.** denotes the number of features with FDR-adjusted p -values that are significant ($p_{adj} < 0.05$), whereas **Task 2 Sig.** indicates the number of features with nominal significance ($p < 0.05$), reported due to the absence of FDR-significant features for Task 2.

Feature Configuration	# Features	Task 1 Sig.	Task 2 Sig.
Static features	99	65	4
Dynamic features	197	123	4
Ratio-based features	253	130	6
Coupling features	203	119	4

aggregated across validation folds to examine whether predictions were driven by a small set of dominant features or by distributed multivariate interactions.

4. Results

4.1. Statistical Results

A summary of statistically significant features across different feature configurations is provided in Table 2. For Task 1, a substantial number of features remained statistically significant after FDR correction. The number of significant features increased as dynamic and normalized descriptors were incorporated. As illustrated in Fig. 1a, the most discriminative features for PVH primarily involved dynamic and higher-order distributional descriptors, exhibiting large effect sizes and consistent group separation. In contrast, for Task 2, no features survived FDR correction under any configuration. Therefore, features with nominal significance ($p < 0.05$) were reported to indicate potential exploratory trends. These findings reveal a notable asymmetry between PVH and NPVH. While PVH can be robustly characterized using univariate statistics, NPVH exhibits minimal separability under the same statistical framework.

4.2. Machine Learning Results

Table 3 shows the classification performance across feature configurations, reported as mean \pm SD over stratified 10-fold CV.

Task 1 (PVH vs. PVH-Control). Task 1 shows consistently high performance across feature configurations. Static features

already yield strong discrimination (AUC = 0.851), and adding dynamic (0.869) and ratio features (0.885) provides incremental gains. The best result is achieved with coupling features using logistic regression (AUC = 0.891 ± 0.04), while the highest F1 is obtained with ratio features (F1 = 0.838).

Task 2 (NPVH vs. Control). Task 2 is substantially more challenging. Static features perform near chance (AUC = 0.556), whereas dynamic features improve AUC to 0.682; ratio features do not consistently help (AUC = 0.608). The strongest performance is achieved with LightGBM-based coupling features (AUC = 0.728 ± 0.10 , F1 = 0.747), although overall separability remains lower than in Task 1.

4.3. Effect of Feature Representations

The results demonstrate a clear asymmetry between the two tasks. For Task 1, performance increases progressively as feature representations become more expressive, indicating that PVH-related differences manifest across static, dynamic, and relational dimensions. In contrast, Task 2 exhibits limited separability under static and ratio-based representations, and only modest improvement when coupling features are introduced.

These findings are consistent with the univariate statistical analysis, where PVH showed robust statistical differences across multiple descriptors, whereas NPVH exhibited minimal separability at the daily summary level. Multivariate modeling partially mitigates this limitation for NPVH but does not close the performance gap observed in Task 1.

4.4. Feature Contribution Analysis

SHAP summary plots for the best-performing model in each task are shown in Fig. 2 and Fig. 3. For Task 1, feature contributions are distributed across both static and dynamic descriptors. Several delta-based statistics (e.g., harmonic variability and upper-tail delta measures) exhibit consistent directional influence on model output. The SHAP value distribution is relatively symmetric and stable, indicating that classification is supported by multiple moderately contributing features rather than a single dominant predictor.

In contrast, Task 2 shows a more concentrated contribution pattern. Dynamic variability measures, particularly higher-

Table 3: Performance (mean \pm standard deviation) over 10-fold cross-validation. Best results for each task are highlighted in bold.

Method	Task 1 (PVH vs PVH-Control)					Task 2 (NPVH vs NPVH-Control)				
	AUC	Acc	Prec	Rec	F1	AUC	Acc	Prec	Rec	F1
Baseline	0.820 [5, 21]	-	-	-	-	0.780 [7]	-	-	-	-
Static	0.851 \pm 0.05	0.811 \pm 0.04	0.851 \pm 0.08	0.818 \pm 0.07	0.828 \pm 0.03	0.556 \pm 0.21	0.552 \pm 0.16	0.594 \pm 0.14	0.689 \pm 0.21	0.631 \pm 0.16
Dynamic	0.869 \pm 0.04	0.821 \pm 0.05	0.869 \pm 0.04	0.801 \pm 0.09	0.831 \pm 0.05	0.682 \pm 0.10	0.640 \pm 0.05	0.660 \pm 0.05	0.800 \pm 0.13	0.715 \pm 0.06
Ratio	0.885 \pm 0.06	0.824 \pm 0.08	0.857 \pm 0.07	0.825 \pm 0.09	0.838 \pm 0.07	0.608 \pm 0.19	0.589 \pm 0.17	0.628 \pm 0.16	0.670 \pm 0.24	0.639 \pm 0.18
Coupling	0.891 \pm 0.04	0.817 \pm 0.05	0.855 \pm 0.04	0.813 \pm 0.11	0.829 \pm 0.06	0.728 \pm 0.10	0.683 \pm 0.05	0.693 \pm 0.04	0.820 \pm 0.11	0.747 \pm 0.05

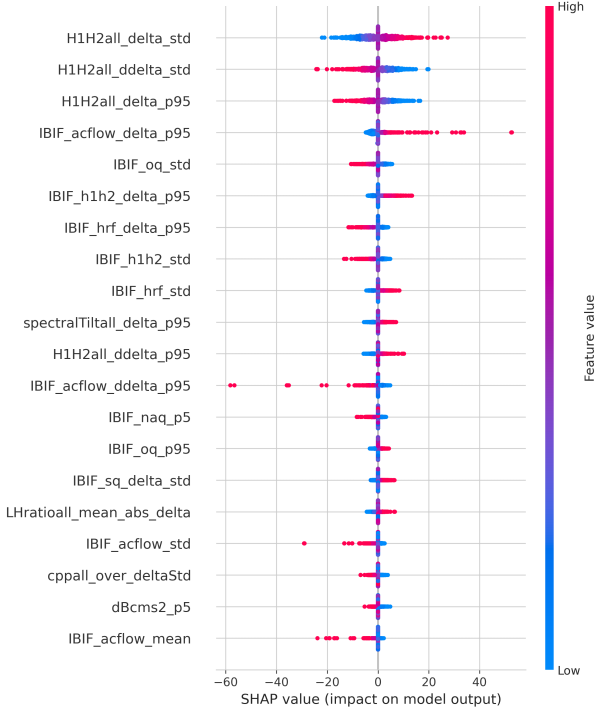


Figure 2: Task 1 SHAP summary (Logistic Regression).

order delta statistics of aerodynamic features (e.g., naq), exhibit stronger localized SHAP magnitudes. The broader spread and higher variance of SHAP values across folds suggest a less stable discriminative structure compared to Task 1.

4.5. Comparison with Univariate Analysis

The multivariate modeling results are consistent with the statistical findings reported earlier. Task 1 demonstrated widespread univariate separability across static, dynamic, and relational descriptors, which translated into robust classification performance across models. Task 2, however, exhibited minimal univariate significance and correspondingly limited classification accuracy. Although nonlinear models partially improved discrimination in Task 2, the overall performance gap between the two tasks remained substantial. These findings indicate that PVH-related ambulatory voice patterns exhibit strong and distributed multivariate structure, whereas NPVH-related patterns show weaker and more interaction-dependent characteristics.

4.6. Performance on the Challenge Held-Out Test Set

Finally, we evaluated our best model on the unseen NeckVibe Challenge test set. For Task 1, we achieved a high discriminative performance with an AUC of **0.917**. This high performance demonstrates the efficacy of the proposed hierarchical feature framework in capturing the complex physiological patterns of phonotraumatic vocal hyperfunction. In contrast, we obtained

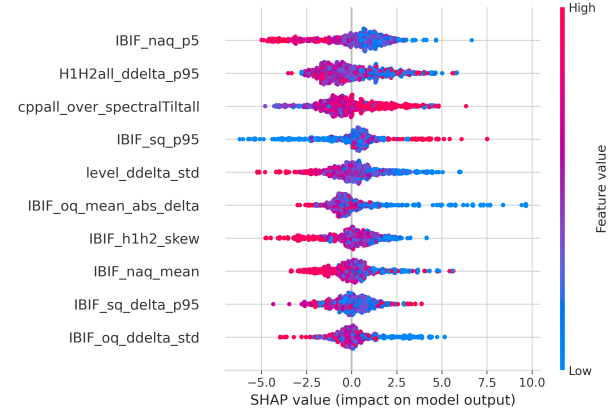


Figure 3: Task 2 SHAP summary (LightGBM).

an AUC of 0.579 in Task 2. This suggests that the pathological contrast in NPVH is insufficiently distinct for multivariate modeling.

5. Discussion and Conclusion

The primary objective of this study was to evaluate the incremental utility of complex feature configurations in characterizing vocal hyperfunction. Our findings reveal a clear divergence in classification performance between Task 1 and Task 2. For Task 1, leveraging coupling features notably enhanced model performance, suggesting that PVH conditions leave distinct physiological signatures in ambulatory voice data. In contrast, the relatively low performance observed in Task 2 reflects a lack of clear discriminatory rationales in the current feature set. In our univariate analysis, no single feature reached statistical significance after FDR correction for NPVH. We hypothesize that NPVH conditions, often characterized by psychological distress or functional imbalances without structural lesions [1, 22], lead to substantial distributional overlap with the control group, making it difficult for models to identify a robust classification boundary using aerodynamic measures.

Although the current NeckVibe Challenge dataset provides feature-level representation only, future work can be considered exploring self-supervised speech models [23, 24] trained on raw waveform data. Such speech foundation models could offer a more nuanced representation of NPVH by modeling raw temporal sequences directly. This approach is particularly promising for NPVH, as its key biomarkers may reside in subtle, non-stationary prosodic variations or micro-tremors in the voice that are often lost during the process of manual feature extraction and temporal averaging [25, 26]. Investigating these high-dimensional latent representations could potentially explore the *hidden* signatures of non-phonotraumatic laryngeal tension and provide a more robust objective assessment tool.

6. Acknowledgement

This research was supported by the InnoCORE program of the Ministry of Science and ICT(GIST InnoCORE KH0860), and by the Regional Innovation System & Education(RISE) program through the Jeonbuk RISE Center, funded by the Ministry of Education(MOE) and the Jeonbuk State, Republic of Korea(2026-RISE-13-WKU).

7. Generative AI Use Disclosure

Generative AI (ChatGPT) was used solely for grammar correction and linguistic polishing of this manuscript. The authors have verified all technical content and maintain full accountability for the work.

8. References

- [1] R. E. Hillman, C. E. Stepp, J. H. Van Stan, M. Zaňartu, and D. D. Mehta, "An updated theoretical framework for vocal hyperfunction," *American Journal of Speech-Language Pathology*, vol. 29, no. 4, pp. 2254–2260, 2020.
- [2] S. Kridgen, R. E. Hillman, T. Stadelman-Cohen, S. Zeitels, J. A. Burns, T. Hron, C. Krusemark, J. Muise, and J. H. Van Stan, "Patient-reported factors associated with the onset of hyperfunctional voice disorders," *Annals of Otolaryngology, Rhinology & Laryngology*, vol. 130, no. 4, pp. 389–394, 2021.
- [3] D. D. Mehta, M. Zanartu, S. W. Feng, H. A. Cheyne II, and R. E. Hillman, "Mobile voice health monitoring using a wearable accelerometer sensor and a smartphone platform," *IEEE Transactions on Biomedical Engineering*, vol. 59, no. 11, pp. 3090–3096, 2012.
- [4] D. D. Mehta, J. H. Van Stan, M. Zaňartu, M. Ghassemi, J. V. Guttag, V. M. Espinoza, J. P. Cortés, H. A. Cheyne, and R. E. Hillman, "Using ambulatory voice monitoring to investigate common voice disorders: Research update," *Frontiers in bioengineering and biotechnology*, vol. 3, p. 155, 2015.
- [5] J. H. Van Stan, D. D. Mehta, A. J. Ortiz, J. A. Burns, L. E. Toles, K. L. Marks, M. Vangel, T. Hron, S. Zeitels, and R. E. Hillman, "Differences in weeklong ambulatory vocal behavior between female patients with phonotraumatic lesions and matched controls," *Journal of Speech, Language, and Hearing Research*, vol. 63, no. 2, pp. 372–384, 2020.
- [6] J. P. Cortés, J. Z. Lin, K. L. Marks, V. M. Espinoza, E. J. Ibarra, M. Zaňartu, R. E. Hillman, and D. D. Mehta, "Ambulatory monitoring of subglottal pressure estimated from neck-surface vibration in individuals with and without voice disorders," *Applied Sciences*, vol. 12, no. 21, p. 10692, 2022.
- [7] J. H. Van Stan, A. J. Ortiz, J. P. Cortes, K. L. Marks, L. E. Toles, D. D. Mehta, J. A. Burns, T. Hron, T. Stadelman-Cohen, C. Krusemark *et al.*, "Differences in daily voice use measures between female patients with nonphonotraumatic vocal hyperfunction and matched controls," *Journal of Speech, Language, and Hearing Research*, vol. 64, no. 5, pp. 1457–1470, 2021.
- [8] M. Zaňartu, J. C. Ho, D. D. Mehta, R. E. Hillman, and G. R. Wodicka, "Subglottal impedance-based inverse filtering of voiced sounds using neck surface acceleration," *IEEE Transactions on Audio, Speech, and Language Processing*, vol. 21, no. 9, pp. 1929–1939, 2013.
- [9] D. D. Mehta, V. M. Espinoza, J. H. Van Stan, M. Zaňartu, and R. E. Hillman, "The difference between first and second harmonic amplitudes correlates between glottal airflow and neck-surface accelerometer signals during phonation," *The Journal of the Acoustical Society of America*, vol. 145, no. 5, pp. EL386–EL392, 2019.
- [10] A. Morales, J. I. Yuz, J. P. Cortés, J. G. Fontanet, and M. Zaňartu, "Glottal airflow estimation using neck surface acceleration and low-order kalman smoothing," *IEEE/ACM transactions on audio, speech, and language processing*, vol. 31, pp. 2055–2066, 2023.
- [11] M. Ghassemi, J. H. Van Stan, D. D. Mehta, M. Zaňartu, H. A. Cheyne II, R. E. Hillman, and J. V. Guttag, "Learning to detect vocal hyperfunction from ambulatory neck-surface acceleration features: Initial results for vocal fold nodules," *IEEE Transactions on Biomedical Engineering*, vol. 61, no. 6, pp. 1668–1675, 2014.
- [12] A. S. Fryd, J. H. Van Stan, R. E. Hillman, and D. D. Mehta, "Estimating subglottal pressure from neck-surface acceleration during normal voice production," *Journal of Speech, Language, and Hearing Research*, vol. 59, no. 6, pp. 1335–1345, 2016.
- [13] Y. Benjamini and Y. Hochberg, "Controlling the false discovery rate: a practical and powerful approach to multiple testing," *Journal of the Royal statistical society: series B (Methodological)*, vol. 57, no. 1, pp. 289–300, 1995.
- [14] K. Jang, L. Li, T.-H. Le, A. Setiani, F. Z. Rami, H. Kim, and Y. C. Chung, "Acoustic biomarkers for schizophrenia spectrum disorders and their associations with symptoms and cognitive functioning," *Progress in Neuro-Psychopharmacology and Biological Psychiatry*, vol. 138, p. 111339, 2025.
- [15] D. R. Cox, "The regression analysis of binary sequences," *Journal of the Royal Statistical Society Series B: Statistical Methodology*, vol. 20, no. 2, pp. 215–232, 1958.
- [16] C. Cortes and V. Vapnik, "Support-vector networks," *Machine learning*, vol. 20, no. 3, pp. 273–297, 1995.
- [17] L. Breiman, "Random forests," *Machine learning*, vol. 45, no. 1, pp. 5–32, 2001.
- [18] T. Chen and C. Guestrin, "Xgboost: A scalable tree boosting system," in *Proceedings of the 22nd acm sigkdd international conference on knowledge discovery and data mining*, 2016, pp. 785–794.
- [19] G. Ke, Q. Meng, T. Finley, T. Wang, W. Chen, W. Ma, Q. Ye, and T.-Y. Liu, "Lightgbm: A highly efficient gradient boosting decision tree," *Advances in neural information processing systems*, vol. 30, 2017.
- [20] S. M. Lundberg and S.-I. Lee, "A unified approach to interpreting model predictions," *Advances in neural information processing systems*, vol. 30, 2017.
- [21] J. P. Cortés, V. M. Espinoza, M. Ghassemi, D. D. Mehta, J. H. Van Stan, R. E. Hillman, J. V. Guttag, and M. Zaňartu, "Ambulatory assessment of phonotraumatic vocal hyperfunction using glottal airflow measures estimated from neck-surface acceleration," *PloS one*, vol. 13, no. 12, p. e0209017, 2018.
- [22] R. E. Hillman, E. B. Holmberg, J. S. Perkell, M. Walsh, and C. Vaughan, "Objective assessment of vocal hyperfunction: An experimental framework and initial results," *Journal of Speech, Language, and Hearing Research*, vol. 32, no. 2, pp. 373–392, 1989.
- [23] A. Baevski, Y. Zhou, A. Mohamed, and M. Auli, "wav2vec 2.0: A framework for self-supervised learning of speech representations," *Advances in neural information processing systems*, vol. 33, pp. 12449–12460, 2020.
- [24] S. Chen, C. Wang, Z. Chen, Y. Wu, S. Liu, Z. Chen, J. Li, N. Kanda, T. Yoshioka, X. Xiao *et al.*, "Wavlm: Large-scale self-supervised pre-training for full stack speech processing," *IEEE Journal of Selected Topics in Signal Processing*, vol. 16, no. 6, pp. 1505–1518, 2022.
- [25] L. B. Helou, W. Wang, R. C. Ashmore, C. A. Rosen, and K. V. Abbott, "Intrinsic laryngeal muscle activity in response to autonomic nervous system activation," *The Laryngoscope*, vol. 123, no. 11, pp. 2756–2765, 2013.
- [26] J.-W. Kim, H. Yoon, B.-N. Kim, S.-Y. Lee, D.-J. Kim, S.-E. Moon, Y. Choi, and C.-M. Yang, "Deep neural network-based analysis of voice biomarkers for monitoring treatment response in adolescent major depressive disorder," *Communications Medicine*, 2026.